Evidence of an inverted hexagonal phase in self-assembled phospholipid-DNA-metal complexes

EUROPHYSICS LETTERS 15 August 2004

Europhys. Lett., **67** (4), pp. 669–675 (2004)
DOI: 10.1209/epl/i2004-10091-y

Evidence of an inverted hexagonal phase in self-assembled phospholipid-DNA-metal complexes

O. Francescangeli[1], M. Pisani[2], V. Stanić[1], P. Bruni[2] and T. M. Weiss[3]

[1] *Dipartimento di Fisica e Ingegneria dei Materiali e del Territorio and INFM Università Politecnica delle Marche - Via Brecce Bianche, 60131 Ancona, Italy*
[2] *Dipartimento di Scienze dei Materiali e della Terra, Università Politecnica delle Marche - Via Brecce Bianche, 60131 Ancona, Italy*
[3] *European Synchrotron Radiation Facility - BP 220, F-38043 Grenoble Cedex, France*

(received 27 April 2004; accepted in final form 7 June 2004)

PACS. 87.14.Cc – Lipids.
PACS. 87.14.Gg – DNA, RNA.
PACS. 61.10.-i – X-ray diffraction and scattering.

Abstract. – We report the first observation of an inverted hexagonal phase of phospholipid-DNA-metal complexes. These ternary complexes are formed in a *self-assembled* manner when water solutions of neutral lipid dioleoylphosphatidylethanolamine (DOPE), DNA and divalent metal cations (Me^{2+}; Me = Fe, Co, Mg, Mn) are mixed, which represents a striking example of supramolecular chemistry. The structure, derived from synchrotron X-ray diffraction, consists of cylindrical DNA strands coated by neutral lipid monolayers and arranged on a two-dimensional hexagonal lattice (H_{II}^c). Besides the fundamental aspects, DOPE-DNA-Me^{2+} complexes may be of great interest as efficient nonviral delivery systems in gene therapy applications because of the low inherent cytotoxicity and the potential high transfection efficiency.

Recent completion of the working draft of the human genome has convinced researchers about the reliable possibility of using gene medicines to combat genetic diseases. It is now well established that the development of gene therapy and genetic engineering is strictly depending on safe and efficient gene delivery vectors. In recent years, several new strategies have been proposed to develop nonviral transfection vectors of DNA for gene therapy. In particular, the condensed complexes between cationic lipids (CLs) and DNA, also known as lipoplexes, have been tested as vehicles for the delivery of DNA into cells, both *in vitro* [1] and *in vivo* [2–4]. The plain advantages shown by lipoplexes include robust manufacture, ease in handling and preparation techniques, low toxicity, ability to link large pieces of DNA and to act as efficient chemical carriers of extracellular DNA across outer cell membranes and nuclear membranes (transfection). A number of studies have shown the existence of a strong correlation between self-assembled structure of CL-DNA complexes and transfection efficiency. Detailed structural measurements, primarily small-angle X-ray scattering (SAXS), freeze-fracture electron microscopy, and cryo-transmission electron microscopy studies, have revealed two major lipoplex geometries, namely lamellar L_α^c and hexagonal H_{II}^c [5–8]. The preferred equilibrium geometry is dictated by a critical interplay between the surface charge

density and the elastic properties of the constituent lipid bilayers [8]. It has been suggested [9], and some evidence exists [8], that inverted hexagonal lipid phases show a higher transfection efficiency, since they are more fusogenic and interact more strongly with the cell membranes.

Extensive effort is being addressed worldwide to the understanding of the various possible self-assembled structures of lipid-DNA complexes. In fact, it is largely accepted that the yet low enhancement of transfection via lipids requires a full understanding of all the possible supramolecular structures of lipid-DNA complexes. Within this frame, our group started recently an extended project focused on the self-assembled association of neutral liposomes (L), DNA and divalent metal cations (Me^{2+}) in triple L-DNA-Me^{2+} complexes [10–13]. The use of neutral lipids should lead to complexes that exhibit lower inherent cytotoxicity than CLs [13–15]. On the other hand, addition of metal cations leads to the formation of complexes that are more stable than binary L-DNA complexes and exhibit higher DNA encapsulation ratios [13,16,17]. The structural and morphological studies of mixtures of dioleoylphosphatidylcholine (DOPC), DNA and Me^{2+} (Me = Mn, Mg, Co, Fe) ions in water solutions have shown the formation of self-assembled DOPC-DNA-Me^{2+} complexes that exhibit the lamellar symmetry of the liquid-crystalline L_α phase [10]. Their structure consists of smectic-like arrays of stacked lipid bilayers with monolayers of DNA molecules intercalated within the intervening water gaps. The experimental results evidenced that the complex formation is promoted by the action of the metal cations that bind the polar heads of DOPC to the negatively charged phosphate groups of DNA, thus showing that neutral liposomes in the presence of metal ions behave similarly to CLs. The formation of such complexes highlights one of the unique properties of lipid membranes, namely, their being self-assembled two-dimensional (2D) fluid mixtures, flexible with respect to curvature deformations.

To test whether the fusogenic action of the metal cations is equally active in promoting and stabilizing triple complexes L-DNA-Me^{2+} from different neutral lipids, we have carried out a SAXS structural study of mixtures of dioleoylphosphatidylethanolamine (DOPE), DNA and divalent metal cations in water solution. In this letter we report the results of this study which provided the first experimental observation of an inverted hexagonal phase of DOPE-DNA-Me^{2+} complexes. It is known that the equilibrium phase of pure DOPE in excess water shows an inverted hexagonal phase, H_{II}, whose structure elements are infinitely long rigid rods, all identical and crystallographically equivalent, regularly packed in a 2D hexagonal lattice. The cylinders are filled by water and are dispersed in the continuous medium constituted by hydrocarbon chains, whereas the polar groups are located at the water-hydrocarbon chain interface. Our study demonstrates the self-assembled formation of ternary DOPE-DNA-Me^{2+} complexes from water mixtures of the three components, revealing a novel inverted-hexagonal structure in which the DNA strands fill the water space inside the cylinders of pure DOPE and the metal cations stabilize the structure by binding the DOPE polar headgroups to the phosphate groups of DNA.

DOPE, DNA from calf thymus (bp = 2675, contour length $\approx 0.9\,\mu$m) and metal ions Mn^{2+}, Mg^{2+}, Co^{2+}, Fe^{2+} as chloride were purchased from Avanti Polar Lipids. Solutions of DNA, DOPE and metal ions were prepared in 4-(2-hydroxyl)piperazine-1-ethanesulphonic acid (HEPES) buffer (20 mM, pH = 7.2). DOPE was first dissolved in chloroform, the solvent was removed under a stream of nitrogen and then vacuum desiccated for two hours in order to remove any trace of solvent. The lipid was hydrated in excess of HEPES solution. The triple DOPE-DNA-Me^{2+} complexes were prepared by adding equal volumes of DOPE (1.75 mM), DNA (2.4 mM) and the metal ion (7 mM) solutions at 3 : 4 : 12 molar ratio. SAXS measurements were carried out at the high-brilliance beamline ID2 at the European Synchrotron Radiation Facility (Grenoble, France). The wavelength of the incident beam was $\lambda = 0.995$ Å (12.5 keV), the beam size was $100\,\mu$m and the sample-to-detector distance was 1.2 m. The

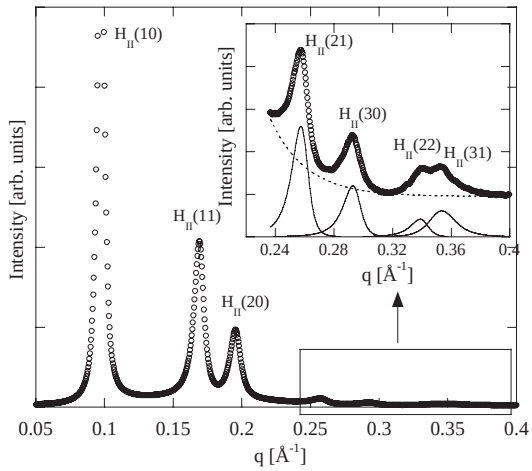

Fig. 1

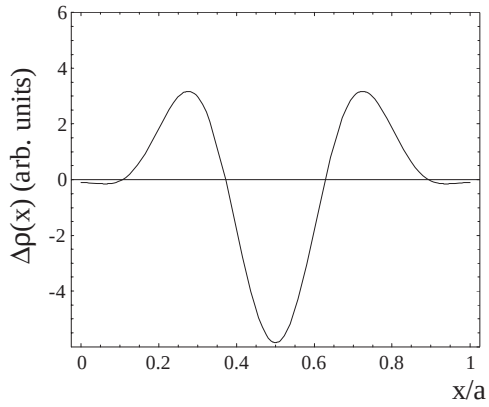

Fig. 2

Fig. 1 – SAXS pattern of DOPE in excess water at $c = 0.14\%$ (symbols are experimental data). The integers in parentheses are Miller indices (hk). The inset shows a view of the higher-q region on an expanded vertical scale. The dashed line is the nonlinear background and the full lines show the fitting functions.

Fig. 2 – The electron density profile of DOPE along the [10] direction of the unit cell. The origin corresponds to the center of the water core.

diffraction patterns were collected by a 2D CCD detector. We investigated the q range from $0.04\,\text{Å}^{-1}$ to $0.5\,\text{Å}^{-1}$ with a resolution of $8 \times 10^{-3}\,\text{Å}^{-1}$ (FWHM). The sample was held in a 1 mm size quartz capillary. Measurements were performed at room temperature, after five hours of incubation time. To avoid radiation damage, a maximum exposure time of 6 s/frame was used for any given sample, a satisfactory statistics being reached by repeating several measurements on fresh samples. The collected 2D powder diffraction spectra were angularly integrated to get 1D intensity *vs.* q patterns. These data were then corrected for the empty sample holder and HEPES bulk solution. In order to calculate the electron density map of DOPE in the H_{II} phase, the integrated intensities of the diffraction peaks were determined by fitting the data with series of Pearson IV functions using a nonlinear baseline. The Lorentz correction was performed by multiplying each integrated intensity by $\sin\theta$ and the intensities were then calibrated by dividing by the multiplicity of the reflection [18, 19]. The square root of the corrected peak was finally used to determine the modulus of the form factor F of each respective reflection. The electron density profile within the unit cell was calculated by Fourier synthesis, which for the $p6$ space group of our hexagonal lattice reads [20]

$$\rho(x,y) = 1/A_{\text{c}}\left[F(00)+2\left\{\sum_{h=1}^{\infty}F_{h,0}\cos(2\pi hx)+\sum_{k=1}^{\infty}F_{0,k}\cos(2\pi ky)\right\}+\right.$$
$$\left.+2\left\{\sum_{h=1}^{\infty}\sum_{k=1}^{\infty}F_{h,k}\cos(2\pi(hx+ky))+\sum_{h=1}^{\infty}\sum_{k=1}^{\infty}F_{-h,k}\cos(2\pi(hx-ky))\right\}\right], \quad (1)$$

where x and y are the coordinates in the unit cell, A_{c} is the area of the unit cell and $F_{h,k}$ is the form factor of the (hk) reflection (a real number, either positive or negative, for centrosymmetric structures). The best phasing choice $(+--+++)$ was obtained following the phasing criteria developed by Harper *et al.* [18].

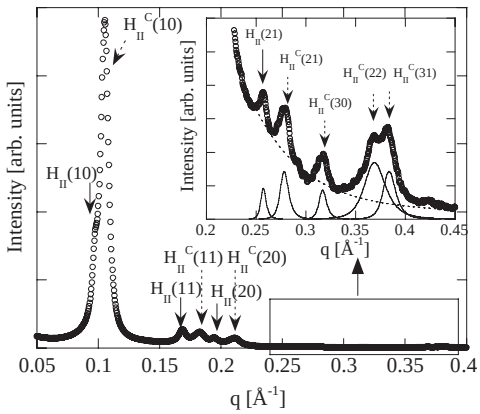

Fig. 3

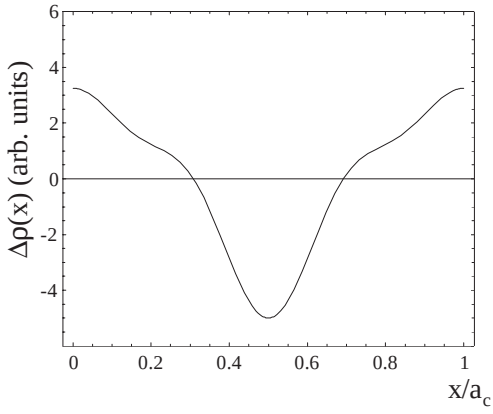

Fig. 4

Fig. 3 – SAXS pattern of the DOPE-DNA-Fe^{2+} complex (3 : 4 : 12). The inset shows the higher-q region on an expanded vertical scale. The dashed line is the nonlinear background and the full lines show the fitting functions.

Fig. 4 – The electron density profile of the DOPE-DNA-Fe^{2+} complex (3 : 4 : 12) along the [10] direction of the unit cell. The origin corresponds to the center of the water core.

The study started with the structural characterization of DOPE in HEPES solution and fig. 1 shows the room temperature (RT) SAXS pattern of DOPE in excess of water (at lipid weight ratio $c = 0.14\%$). Bragg peaks up to the seventh order are observed which can be indexed perfectly on a 2D hexagonal lattice with a unit cell spacing of $a = 74.4$ Å, according to the equation $q_{hk} = 4\pi(h^2 + kh + k^2)^{1/2}/\sqrt{3}a$. This pattern corresponds to the well-known 2D columnar inverted hexagonal phase, H_{II}, of DOPE [19]. Figure 2 shows the electron density (ED) profile along the [10] direction, $\Delta\rho = \rho - \langle\rho\rangle$, where $\langle\rho\rangle$ is the average of ρ over the unit cell. This function gives information on the internal structure of the unit cell. The two ED maxima correspond to the polar headgroups and the central minimum to the hydrocarbon chain region. The distance between the centers of the density maxima gives the phosphate-to-phosphate group distance $d_{\mathrm{PP}} = 33.2$ Å. However, this value underestimates the steric lipid bilayer thickness, d_{L}, because of the finite width of the headgroups [19, 21]. A more reliable value of d_{L} was obtained by estimating the width of the headgroup, d_{H}, through the ED *Cylindrical Modelling* procedure described in ref. [19]. This calculation gave $d_{\mathrm{H}} = 11.0$ Å, hence $d_{\mathrm{L}} = d_{\mathrm{PP}} + d_{\mathrm{H}} = 44.2$ Å and the average diameter of the water core $d_{\mathrm{w}} = 2R_{\mathrm{w}} = a - d_{\mathrm{L}} = 30.2$ Å.

Figure 3 shows the RT diffraction pattern of DOPE-DNA-Fe^{2+} complex at 3 : 4 : 12 molar ratio (for the corresponding ED, cf. fig. 4). Two distinct sets of peaks are identified, labeled as H_{II} and H_{II}^{c}, which can be indexed on 2D hexagonal lattice with different unit cell spacings, namely $a = 74.5$ Å and $a_{\mathrm{c}} = 68.7$ Å, respectively. The first set of peaks corresponds to the H_{II} phase of pure DOPE, whereas the second set is consistent with the 2D columnar inverted hexagonal structure shown in fig. 5, which we refer to as the H_{II}^{c} phase of phospholipid-DNA-Me^{2+} complexes, where the DNA strands are surrounded by a lipid monolayer, with the DNA-lipid inverted cylindrical micelles arranged on a hexagonal lattice. The hexagonal phase of the complex was confirmed by the freeze-fracture electron microscopy (FF-EM) analysis. As an example, fig. 6 shows the FF-micrograph of DOPE-DNA-Fe^{2+} (3 : 4 : 12) where the striation pattern (due to elongated cylinders) typical of hexagonal lipid structures is

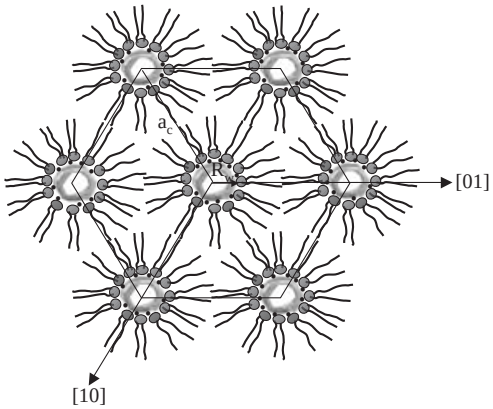

Fig. 5

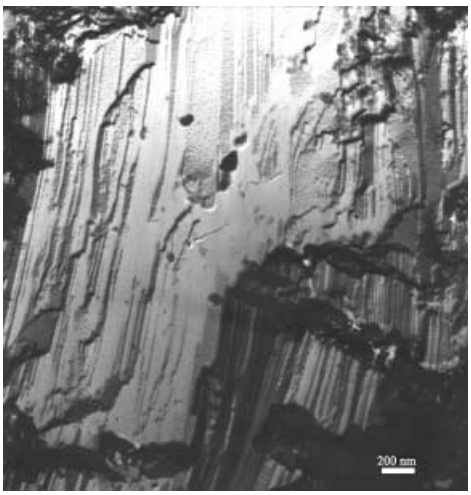

Fig. 6

Fig. 5 – Cross-section of the H_{II}^c phase of DOPE-DNA-Me^{2+} complexes. The unit cell of the hexagonal lattice is also shown.

Fig. 6 – Freeze-Fracture micrograph of DOPE-DNA-Fe^{2+} complex, the striation pattern is characteristic in hexagonal lipid structures.

apparent. The structure of the H_{II}^c phase resembles that of the H_{II} phase of pure DOPE in excess water, with the water space inside the lipid micelle filled by DNA. The presence of Bragg peaks up to the seventh order indicates a high degree of regularity of the structure. The relative suppression of the (11) and (20) peak intensities compared with that in the H_{II} phase of the DOPE is the diffraction signature of the greater electron density of DNA with respect to water. This is confirmed by the electron density profile of the H_{II}^c phase along the [10] direction, shown in fig. 4. The two shoulders observed at $x/a_c \cong 0.26$ and $x/a_c \cong 0.73$ correspond to the phosphorus and may be used to localize the centers of the polar headgroups. From the structural data of fig. 5 and following the procedure previously described for pure DOPE, we could estimate $d_{PP} = 32.6\,\text{Å}$, $d_L = 43.6\,\text{Å}$, hence the water layer thickness $d_w = 2R_w = a_c - d_L = 25.1\,\text{Å}$. This value is large enough to accommodate a double-stranded DNA molecule surrounded by one hydration layer [22]. The simultaneous presence of the two sets of peaks in the diffraction pattern indicates coexistence of the H_{II} and of pure DOPE and DOPE-DNA-Fe^{2+} complex, respectively. The structure of fig. 5 is similar to that observed in CL-DNA complexes containing DOPE [8]. There, the cylindrical concentric geometry allowed neutralization of the DNA charges by the cationic surface charges through direct electrostatic interactions. Unlike cationic lipoplexes, in our complexes DNA-DOPE interactions are mediated by the bivalent metal cations. There are two possibilities for DOPE-DNA-Me^{2+} binding. The first option is for the metal cation to bridge the phosphate on the lipid headgroup (mainly oriented with the phosphate closest to the lipid/water interface) with a phosphate on DNA. The second option consists in a neutralization between the bivalent cation and two phosphate groups in two different DOPE units followed by a reorientation of the DOPE headgroups with the positively charged amine pointing toward the DNA. In the latter case, the metal and the lipid should form a new bridging unit and acquire cationic properties as postulated for the complex DPPC-DNA-Ca^{2+} [9]. The situation is different in the case of DOPE, because different ionic structures can be obtained depending on *p*H. Considering

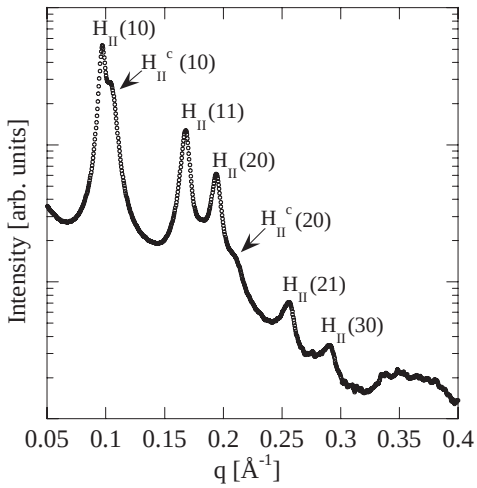

Fig. 7

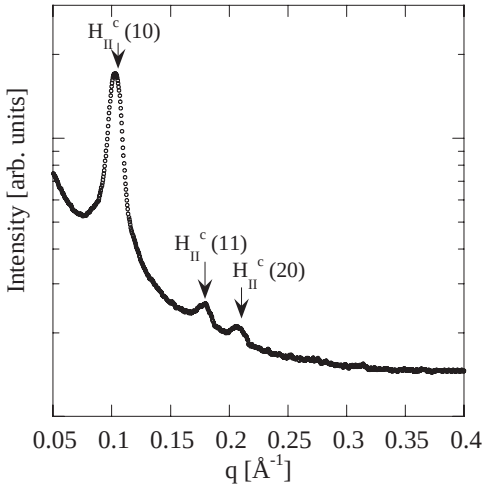

Fig. 8

Fig. 7 – SAXS pattern showing the coexistence of the DOPE and DOPE-DNA-Mn^{2+} structures (3 : 4 : 12).

Fig. 8 – SAXS pattern of the DOPE-DNA-Co^{2+} complex (3 : 4 : 12) after long incubation time (48 h).

that ethanolamine shows a $p\mathrm{K}_a = 9.5$, one should assume that DOPE at $p\mathrm{H} = 7.5$ is in the negative form; this means that metal cations must bridge the negative phosphate of DNA and of DOPE to allow complexation. In consequence, the resulting interaction is of the type described in the first option. Further investigations, mainly based on measures at different pH, are needed to eventually support this option. In the lack of more appropriate data, it seems reasonable that the driving force for DNA-lipid complexation in the presence of metal cations is (almost mainly) due to the release of counterion entropy upon neutralization of DNA phosphate groups [23], also in the hypothesis that the mechanism based on negative DOPE was operating.

Similar results were observed for the complexes with other metal cations (Co^{2+}, Mn^{2+}, Mg^{2+}). A representative example is reported in fig. 7 for the RT diffraction pattern of DOPE-DNA-Mn^{2+} (3 : 4 : 12) while the full set of data will be reported elsewhere. Coexistence of the two inverse hexagonal structures of the complex and the pure DOPE is apparent, with lattice parameters $a_\mathrm{c} = 69.3$ Å and $a = 74.8$ Å, respectively. The lower number of higher diffraction orders indicates a reduced degree of regularity of the structure compared to that of the Fe^{2+} complex.

The relative volume concentrations of the two coexisting hexagonal structures depend on several variables such as incubation time, temperature, water dilution and molar ratios of the components. As an example, fig. 8 shows the RT diffraction pattern of DOPE-DNA-Co^{2+} (3 : 4 : 12) after very long incubation time (48 hours). Only the diffraction signature of the H_{II}^c phase is observed, with $a_\mathrm{c} = 70.2$ Å, which means that in those conditions the process of DNA condensation into the H_{II}^c phase involves the overall DOPE. A more general study of this dependence goes beyond the purposes of the present paper and will be the subject of future investigations.

In conclusion, we have found that water solutions of DOPE and divalent metal cations can condense DNA into a novel inverse hexagonal structure, H_{II}^c, in which DNA strands are surrounded by a lipid monolayer and the resulting DNA-lipid inverted cylindrical mi-

celles are regularly arranged on a 2D hexagonal lattice. This process of self-aggregation into ternary DOPE-DNA-Me^{2+} complexes is driven by the release of counterion entropy upon neutralization of the DNA phosphate groups operated by the metal cations, either directly or indirectly. We believe that, besides the fundamental interest, the presented results may be of interest from an applicative point of view. In fact, because of the lower inherent cytotoxicity of complexes based on neutral lipids and the higher intrinsic transfection efficiency of the columnar hexagonal structure compared to the lamellar L_α structure of conventional lipoplexes, DOPE-DNA-Me^{2+} complexes could find applications as efficient nontoxic DNA vectors in gene therapy.

REFERENCES

[1] Felgner P. L., Gadek T. R., Holm M., Roman R., Chan H. W., Wenz M., Northrop J. P., Ringold G. M. and Danielsen M., *Proc. Natl. Acad. Sci. USA*, **84** (1987) 7413.
[2] Fortunati E., Bout A., Zanta M. A., Valerio D. and Scarpa M., *Biochim. Biophys. Acta*, **62** (1996) 1306.
[3] Lee E. R., Marshall J., Siegel C. S., Jiang C., Yew N. S., Nicholos M. R., Nietupski J. B., Ziegler R. J., Lane M. B., Wang K. X., Wan N. C., Scheule R. K., Harris D. J., Smith A. E. and Cheng S. H., *Hum. Gene. Ther.*, **7** (1996) 1701.
[4] Templeton N. S., Lasic D. D., Frederik P. M., Strey H. H., Roberts D. D. and Pavlakis G. N., *Nature Biotech.*, **15** (1997) 647.
[5] Sternberg B., Sorgi F. L. and Huang L., *FEBS Lett.*, **356** (1994) 361.
[6] Rädler J. O., Koltover I., Salditt T. and Safinya C. R., *Science*, **275** (1997) 810.
[7] Lasic D. D., Strey H., Stuart M. C. A., Podgornik R. and Frederik P. M., *J. Am. Chem. Soc.*, **119** (1997) 832.
[8] Koltover I., Salditt T., Rädler J. O. and Safinya C. R., *Science*, **281** (1998) 78.
[9] McManus J. J., Rädler J. O. and Dawson K. A., *J. Phys. Chem. B*, **107** (2003) 9869.
[10] Francescangeli O., Stanic V., Gobbi L., Bruni P., Iacussi M., Tosi G. and Bernstorff S., *Phys. Rev. E.*, **67** (2003) 011904.
[11] Francescangeli O., Pisani M., Stanic V., Bruni P. and Iacussi M., *Recent Res. Devel. Macromol.*, **7** (2003) 247.
[12] Francescangeli O., Stanic V., Lucchetta D. E., Bruni P., Iacussi M. and Cingolani F., *Mol. Cryst. Liq. Cryst.*, **398** (2003) 259.
[13] Pott T. and Roux D., *FEBS Lett.*, **511** (2002) 150.
[14] Chonn A., Cullic P. R. and Devine D. V., *J. Immunol.*, **146** (1991) 4234.
[15] Malone R. (Editor), *Non-viral Genetic Therapeutics; Advances Challenges and Applications for Self-Assembling Systems*, Vol. **9** (IBC's Library Series, Boston, Mass.) 1995.
[16] Koiv A., Palvimo J. and Kinnunen P. K. J., *Biochem.*, **34** (1995) 8018.
[17] Fedorov B. B., D'yachkov P. N. and Zhandov R. J., *Russ. Chem. Bull.*, **48** (1999) 2046.
[18] Harper P. E., Rau D. C. and Parsegian W. A., *Macromolecules*, **22** (1989) 1780.
[19] Turner D. C. and Gruner S. M., *Biochemistry*, **31** (1992) 1340.
[20] *International Tables for X-ray Crystallography*, Vol. **I** (The Kynoch Press, Birmingham) 1969.
[21] Rappolt M., Nickel A., Bringezu F. and Lohner K., *Biophys. J.*, **84** (2003) 3111.
[22] Podgornik R., Nickel A., Bringezu F. and Lohner K., *Biophys. J.*, **84** (2003) 3111.
[23] Podgornik R. *et al.*, in *Gene and Cell Therapy: Therapeutic Mechanisms and Strategies*, edited by Templeton N. S. (Marcel Dekker, Inc., New York) 2003.